Available online at www.sciencedirect.com
SCIENCE DIRECT®
Performance Evaluation 59 (2005) 225–246
PERFORMANCE EVALUATION
An International Journal
www.elsevier.com/locate/peva

An analytical model for CDMA downlink rate optimization taking into account uplink coverage restrictions

A. Irwan Endrayanto[a,*], Hans van den Berg[b,c], Richard J. Boucherie[a]

[a] *Department of Applied Mathematics, Stochastic Operations Research Group, University of Twente, P.O. Box 217, 7500 AE Enschede, Netherlands*
[b] *Department of Computer Science, Design and Analysis of Communication Systems Group, University of Twente, P.O. Box 217, 7500 AE Enschede, Netherlands*
[c] *TNO Telecom, P.O. Box 5050, 2600 GB Delft, Netherlands*

Available online 11 September 2004

Abstract

This paper models and analyzes downlink and uplink power assignment in code division multiple access (CDMA) mobile networks. By discretizing the area into small segments, the power requirements are characterized via a matrix representation that separates user and system characteristics. We obtain a closed-form analytical expression of the so-called Perron–Frobenius eigenvalue of that matrix, which provides a quick assessment of the feasibility of the power assignment for each distribution of calls over the segments. Our results allow for a fast evaluation of outage and blocking probabilities. The result also enables a quick evaluation of feasibility that may be used for capacity allocation. Our combined downlink and uplink feasibility model is applied to determine maximal system throughput in terms of downlink rates.

Keywords: CDMA; Capacity allocation; Feasibility power assignment; Discretized cells model; Perron–Frobenius eigenvalue

* Corresponding author.
E-mail addresses: a.i.endrayanto@math.utwente.nl (A.I. Endrayanto), j.l.vandenberg@utwente.nl, j.l.vandenberg@telecom.tno.nl (H. van den Berg), r.j.boucherie@utwente.nl (R.J. Boucherie).

0166-5316/$ – see front matter © 2004 Elsevier B.V. All rights reserved.
doi:10.1016/j.peva.2004.07.004

1. Introduction

The third generation Universal Mobile Telecommunications System (UMTS) employees code division multiple access (CDMA) as the technique of sharing the network capacity among multiple terminals. In a CDMA system, transmissions of different terminals are separated using (pseudo) orthogonal codes. The impact of multiple simultaneous calls is an increase in the interference level, that limits the capacity of the system. The assignment of transmission powers to calls is an important problem for network operation, since the interference caused by a call is directly related to that power.

In a CDMA system the uplink (mobile terminal to base transmitter station (BTS)) and downlink (BTS to mobile) have different characteristics, and must be analyzed separately. The uplink determines coverage, whereas the downlink determines capacity. As the downlink has more capacity (due to e.g. a higher transmit power of the BTSs), in many studies the uplink has been investigated in detail. A successful analytical uplink concept is the effective interference model developed by [7], which enables a fast evaluation of network state feasibility. However, the analysis in [7] requires a homogeneous distribution of the users over the network cells. In [8], feasibility is characterized via the Perron–Frobenius eigenvalue of an interference matrix of the network state. Unfortunately, for the uplink the PF eigenvalue is not available in closed-form so that it provides only a semi analytical evaluation of the uplink capacity. For the downlink most studies are based on pole capacity [17] or based on discrete event or Monte-Carlo simulation leading to slow evaluation of feasibility and/or capacity [20].

The objective of this paper is to develop an analytical model that allows a fast evaluation of the downlink feasibility of CDMA under non-homogeneous traffic load. In particular, we aim for an analog of the uplink effective interference model. Furthermore, we develop a feasibility model for determining the optimal border location. The approach is based on maximizing the total utility of system. This is different from the power allocation minimization problem discussed in some papers (see e.g., [19,22,4,3]). Those papers focused on the optimality in power control and rate assignments. A different type of optimality was proposed in [18] where the optimality is based on maximizing the social welfare of the system of a single cell. In this paper, we also aim to develop a model for analyzing the border location optimality based on the feasibility model.

We focus on modelling BTSs located along a highway to include both non-homogeneity of the call distribution, and mobility of calls. Users are located in cars passing through the cells. Due to e.g. traffic jams (“hot spots”) the load of the cells will not be distributed evenly along the road. To characterize the distribution of a single type of calls in the cells, we propose a discretized-cell model. Each cell is divided into small segments. Then, the nonhomogeneous load can be characterized by the mean number of calls and fresh call arrival rates in the segments. Taking into account interference between segments in neighboring cells and between segments within the cells, we express the generated downlink interference per segment towards the other segments in a matrix form. The resulting matrix characterizes the feasibility of each call configuration, which can be determined by investigating the Perron–Frobenius (PF) eigenvalue of the matrix. Furthermore, a state space of feasible call configurations over the segments is defined, and two performance measures, the outage and blocking probability, are derived from our model. The model is also used to determine the optimal cell border in downlink CDMA. The applicability of our result is illustrated by some numerical examples, in particular focusing in optimal downlink rate allocation taking into account both uplink and downlink feasibility.

The remainder of this paper is organized as follows. Section 2 describes downlink and uplink interference models for persistent and non persistent calls. The performance analysis is presented in Section 3. In

Section 4, we develop a combined down- and uplink capacity allocation model. In Section 5 we present the numerical results, and, finally, in Section 6 we summarize our work and draw conclusions.

2. Model

This paper focuses on a CDMA system consisting of BTSs located along a highway. For simplicity, as we are primarily interested in the interaction between mobility of users along a road and the teletraffic behavior of our wireless network, we focus on a two cell model, where only the area in between two base stations is taken into account. The description can readily be generalized to larger networks.

Consider a linear network model consisting of two BTSs, X and Y, say. Let the area between these BTSs be divided into segments of length δ. For the description below, we fix the radii of the cells. Let cell X resp. Y contain I resp. J segments, labelled $i = 1, \ldots, I$, $j = 1, \ldots, J$, respectively. Then $L_1 = I\delta$ is the radius of cell X, see Fig. 1. Let $D = \delta(I + J)$, the distance between the BTSs. We assume that the segments are small, so that we may approximate the location of subscribers in a segment to be in the middle of that segment, i.e. for segment i of cell X, users are located at distance $i^* = \delta[(i-1) + i]/2$ from X. In this paper, we assume that the propagation model between a transmitter and a receiver is [9]

$$P_i = P_0(d_i)^{-\gamma}, \tag{1}$$

where P_i is the received power, P_0 the transmitted power, d_i the distance between transmitter and receiver and γ the path loss exponent.

2.1. Persistent calls

A common measure for the quality of the transmission is the energy per bit to interference ratio, (E_b/I_0), that for the downlink terminal u, say, is defined as (see e.g. [7,9]).

$$\left(\frac{E_b}{I_0}\right)_u = \frac{W}{R}\frac{\text{useful signal power received by user u}}{(\text{interference power} + \text{thermal noise})}, \tag{2}$$

where W is the system chip rate and R is the data rate. We consider a single terminal type, where all terminals have the same downlink data rate R_D and the same uplink data rate R_U. The interference model for downlink and uplink are different: for the downlink a few BTSs transmit to many terminals, where as for the uplink, many terminals transmit to a few BTSs.

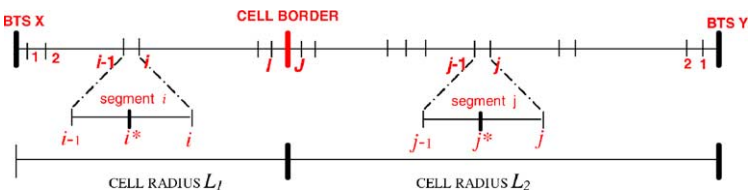

Fig. 1. Discretized cell model.

2.1.1. Downlink model

In our discretized model, let X_i resp. Y_j be the transmit power of BTS X resp. Y to terminals x_i resp. y_j located in segments i resp. j (located at point i^* resp. j^*) of cells X resp. Y. Downlink transmission at sufficient quality requires the energy per bit to interference ratio of a terminal in segment i, $(E_b/I_0)_i^{\text{Down}}$, to exceed a certain threshold ϵ_D^*, i.e., a terminal in segment i requires the BTS to transmit enough power such that

$$\frac{W}{R_D}\frac{X_i(i^*)^{-\gamma}}{(D-i^*)^{-\gamma}\sum_{j=1}^{J} m_j Y_j + \alpha(i^*)^{-\gamma}\left(\sum_{l=1}^{I} n_l X_l - X_i\right) + N_0} \geqslant \epsilon_D^*, \tag{3}$$

where n_i resp. m_j are the number of terminals in segment i resp. j of cell X resp. Y, α is non-orthogonality factor and N_0 is the thermal noise level. This expression can be rearranged as

$$X_i \geqslant \Gamma_D\left(\left(\frac{D-i^*}{i^*}\right)^{-\gamma}\sum_{j=1}^{J} m_j Y_j + \alpha\left(\sum_{l=1}^{I} n_l X_l - X_i\right) + N_0\left(\frac{1}{i^*}\right)^{-\gamma}\right), \tag{4}$$

where $\Gamma_D = \epsilon_D^*(R_D/W)$. By analogy, we also can express the required transmitted power Y_j of BTS Y to user y_j located in segment j of cell Y. The resulting system of Eq. (4) is

$$\begin{cases} s\mathbf{I}_X\mathbf{X} \geqslant \Gamma_D\mathbf{P}_X\mathbf{1}_Y\mathbf{M}\mathbf{Y} + \alpha\Gamma_D\mathbf{1}_X\mathbf{N}\mathbf{X} + \Gamma_D N_0\mathbf{D}_X \\ s\mathbf{I}_Y\mathbf{Y} \geqslant \Gamma_D\mathbf{P}_Y\mathbf{1}_X\mathbf{N}\mathbf{X} + \alpha\Gamma_D\mathbf{1}_Y\mathbf{M}\mathbf{Y} + \Gamma_D N_0\mathbf{D}_Y \end{cases} \tag{5}$$

where $s = 1 + \alpha\Gamma_D$, $\mathbf{X} = (X_1\, X_2 \ldots X_I)^T$, $\mathbf{Y} = (Y_1\, Y_2 \cdots Y_J)^T$ represent the transmit powers to the segments; $\mathbf{N} = \text{diag}(n_i)$ the diagonal matrix of size $I \times I$ that represents the number of terminals in each segment in cell X, and similarly $\mathbf{M} = \text{diag}(m_i)$ is a diagonal matrix of size $J \times J$ that represents the number of terminals in each segment in cell Y; $\mathbf{P}_X = (p_{ij}^X)$, where $p_{ij}^X = (D - i^*/i^*)^{-\gamma}$ the matrix of size $I \times J$ that represents the inter-cell path loss from segment j in cell Y and segment i in cell X, and similarly $\mathbf{P}_Y = (p_{ji}^Y)$, where $p_{ji}^Y = (D - j^*/j^*)^{-\gamma}$; $\mathbf{D}_X = ((1/1^*)^{-\gamma}(1/2^*)^{-\gamma} \cdots (1/I^*)^{-\gamma})^T$, $\mathbf{D}_Y = ((1/1^*)^{-\gamma}(1/2^*)^{-\gamma} \cdots (1/J^*)^{-\gamma})^T$ representing the intra-cell path loss from the BTS to segments within the cell; $\mathbf{I}_X$ (and $\mathbf{I}_Y$) be the identity matrix of size $I \times I$ ($J \times J$) and $\mathbf{1}_X$ ($\mathbf{1}_Y$) is a matrix of size $I \times I$ ($J \times J$) with all entries equal to 1.

This system can be rewritten as

$$(s\mathbf{I} - \mathbf{T})\mathbf{Z}^D \geqslant \mathbf{c}, \tag{6}$$

where

$$\mathbf{I} = \begin{pmatrix} \mathbf{I}_X & \mathbf{0} \\ \mathbf{0} & \mathbf{I}_Y \end{pmatrix}; \quad \mathbf{T} = \begin{pmatrix} \alpha\Gamma_D\mathbf{1}_X\mathbf{N} & \Gamma_D\mathbf{P}_X\mathbf{M} \\ \Gamma_D\mathbf{P}_Y\mathbf{N} & \alpha\Gamma_D\mathbf{1}_Y\mathbf{M} \end{pmatrix}; \quad \mathbf{Z}^D = \begin{pmatrix} \mathbf{X} \\ \mathbf{Y} \end{pmatrix}; \quad \mathbf{c} = N_0\Gamma_D\begin{pmatrix} \mathbf{D}_X \\ \mathbf{D}_Y \end{pmatrix}$$

The system (6) is the downlink power control equation. If (6) has a non-negative solution then a feasible power assignment can be found. Notice that under perfect power control, the system (6) is satisfied with equality, see [8]. We further investigated feasibility in Section 3.1.

2.1.2. Uplink model

Consider the uplink in our discretized cell model. Let X_i^{R} resp. Y_j^{R} be the received power at BTS X resp. Y from terminals x_i resp. y_j in segments i resp. j (at points i^* resp. j^*) of cells X resp. Y. Uplink transmission at sufficient quality requires the energy per bit to interference ratio of a terminal in segment i at the BTS, $(E_{\mathrm{b}}/I_0)_i^{\mathrm{Up}}$, to exceed a certain threshold ϵ_{U}^*, i.e.,

$$\frac{W}{R_{\mathrm{U}}}\frac{X_i^{\mathrm{R}}}{(\sum_{j=1}^{J} m_j Y_j^{\mathrm{R}}(D-j^*/j^*)^{-\gamma})+\sum_{k=1}^{I} n_k X_k^{\mathrm{R}} - X_i^{\mathrm{R}} + N_0} \geqslant \epsilon_{\mathrm{Up}}^*. \tag{7}$$

Under the assumption of perfect power control, BTS X requires all terminals in the cell to transmit enough power such that the received signal is the same, i.e., $X_i^{\mathrm{R}} = X^{\mathrm{R}}$ and $Y_j^{\mathrm{R}} = Y^{\mathrm{R}}$ (see e.g. [9]). Thus, the received signal should satisfy

$$X^{\mathrm{R}} \geqslant \Gamma_{\mathrm{U}}\left(Y^{\mathrm{R}}\left(\sum_{j=1}^{J} m_j p_j\right) + X^{\mathrm{R}}(N-1) + N_0\right), \tag{8}$$

where $N = \sum_{k=1}^{I} n_k$ and $p_j = (D - j^*/j^*)^{-\gamma}$ and $\Gamma_{\mathrm{U}} = \epsilon_{\mathrm{U}}^*(R_{\mathrm{U}}/W)$. A similar system can be derived for BTS Y. Combine these two inequalities, we have the following uplink feasibility condition:

$$(\mathbf{I} - \mathbf{H})\mathbf{Z}^{\mathrm{U}} \geqslant \mathbf{c}, \tag{9}$$

where

$$\mathbf{H} = \begin{pmatrix} \Gamma_{\mathrm{U}}(N-1) & \Gamma_{\mathrm{U}}\sum_{j=1}^{J} m_j p_j \\ \Gamma_{\mathrm{U}}\sum_{i=1}^{I} n_i p_i & \Gamma_{\mathrm{U}}(M-1) \end{pmatrix}; \quad \mathbf{Z}^{\mathrm{U}} = \begin{pmatrix} X^{\mathrm{R}} \\ Y^{\mathrm{R}} \end{pmatrix}; \quad \mathbf{c} = \Gamma_{\mathrm{U}} N_0 \begin{pmatrix} 1 \\ 1 \end{pmatrix}.$$

2.2. Non-persistent and moving calls

Consider the discretized linear wireless network with non-persistent and moving users. Let fresh calls arrive according to a Poisson arrival process with rate proportional to the density of terminals along the road, and let terminals move along the road according to the laws of road traffic movement.

The prediction of the location of subscribers used in this paper requires an estimate of the density of terminals. For the purpose of this paper, a simplified model as provided in [13] is sufficient. Let $k(x, t)$ denote the density of terminals at location x at time t. Then the traffic mass conservation principle states that

$$\frac{\partial k(x,t)}{\partial t} + \frac{\partial k(x,t)v(x,t)}{\partial x} = 0, \tag{10}$$

where $v(x, t)$ is the velocity on location x at time t.

In a mobile network the number of terminals making a call is typically substantially smaller than the number of terminals not making a call. Therefore, it is natural to assume that *fresh calls* in segment i are generated according to a Poisson process with non-stationary arrival rate

$$\beta_i(t) := \beta \int_{r_i}^{r_{i+1}} k(x,t)\,\mathrm{d}x, \tag{11}$$

proportional to the density of traffic in segment i at time t, where β is the arrival rate of fresh calls per unit traffic mass, and r_i and r_{i+1} are the borders of segment i. Let the call lengths be independent and identically distributed random variables, with common distribution G and mean τ independent of the location and traffic density.

3. Performance analysis

In this section, we first establish downlink and uplink feasibility for persistent calls via the Perron–Frobenius (PF) eigenvalues of the matrix $\mathbf{T}$ and $\mathbf{H}$, that is explicitly provided in Section 3.1. Section 3.2 considers the model with non-persistent calls and discusses the time-dependent distribution of calls over the segments, and corresponding blocking and outage probabilities.

3.1. Persistent calls: feasibility

Feasibility of the power assignment for the downlink and uplink are characterized by the matrix inequalities (6) and (9), resp. In this section, by analogy with [8], we investigate feasibility via theory of non-negatives matrices [16].

3.1.1. Downlink feasibility

Under the assumption of perfect power control, if $(s\mathbf{I} - \mathbf{T})\mathbf{Z}^{\mathrm{D}} \geqslant \mathbf{c}$ then the equation is satisfied with equality, i.e., $(s\mathbf{I} - \mathbf{T})\mathbf{Z}^{\mathrm{D}} = \mathbf{c}$. According to the Perron–Frobenius theorem in [16], feasibility is then determined by the Perron–Frobenius (PF) eigenvalue $\lambda(\mathbf{T})$ of the matrix $\mathbf{T}$, i.e.,

$$\mathbf{Z}^{\mathrm{D}} \geq \mathbf{0} \text{ exist and } \mathbf{Z}^{\mathrm{D}} = (s\mathbf{I} - \mathbf{T})^{-1}\mathbf{c} \Longleftrightarrow \lambda(\mathbf{T}) < s. \tag{12}$$

Thus, downlink feasibility of our cellular system is characterized by the matrix $\mathbf{T}$, where the distribution of calls over the segments appears in $\mathbf{T}$. The system and user characteristics in this matrix can be separated as

$$\mathbf{T} = \begin{pmatrix} \alpha\Gamma_{\mathrm{D}}\mathbf{1}_X & \Gamma_{\mathrm{D}}\mathbf{P}_X \\ \Gamma_{\mathrm{D}}\mathbf{P}_Y & \alpha\Gamma_{\mathrm{D}}\mathbf{1}_Y \end{pmatrix} \begin{pmatrix} \mathbf{N} & 0 \\ 0 & \mathbf{M} \end{pmatrix} = \mathbf{SU}, \tag{13}$$

where

$$\mathbf{U} = \begin{pmatrix} \mathbf{N} & 0 \\ 0 & \mathbf{M} \end{pmatrix},$$

represents the distribution of the number of calls in each segment, and

$$\mathbf{S} = \begin{pmatrix} \alpha\Gamma_{\mathrm{D}}\mathbf{1}_X & \Gamma_{\mathrm{D}}\mathbf{P}_X \\ \Gamma_{\mathrm{D}}\mathbf{P}_Y & \alpha\Gamma_{\mathrm{D}}\mathbf{1}_Y \end{pmatrix}$$

contains the system parameters. The entries of $\mathbf{S}$ are fixed for given system parameters. Thus $\lambda(\mathbf{T})$ is determined by the distribution of calls over the segments, i.e., $\lambda(\mathbf{T}) := \lambda(\mathbf{U})$.

The characterization (12) provides a clear motivation for the discretization into segments as we obtain a downlink interference model that is very similar to uplink models such as studied in [2,7,8] where feasibility of the uplink power control algorithm is characterized via the Perron–Frobenius (PF) eigenvalue of a matrix containing the number of calls in the cell (not in segments). Effective interference models such as developed in [7] allow for a characterization of feasibility based on that total number only, but they assume a homogeneous distribution of calls over the area covered by a cell.

The following theorem provides an explicit expression of PF eigenvalue of matrix $\mathbf{T}$.

Theorem 1. *The Perron–Frobenius eigenvalue of* $\mathbf{T}$ *is*

$$\lambda(\mathbf{T}) = \frac{\Gamma}{2}\alpha\left(\sum_{i=1}^{I} n_i + \sum_{j=1}^{J} m_j\right) + \frac{\Gamma}{2}\sqrt{\alpha^2\left(\sum_{i=1}^{I} n_i - \sum_{j=1}^{J} m_j\right)^2 + 4\sum_{i=1}^{I} p_i n_i \sum_{j=1}^{J} p_j m_j}. \tag{14}$$

Proof. The PF eigenvalue of matrix T is determined from the characteristic polynomial of matrix $\mathbf{T}$, i.e., $|\mathbf{T} - \lambda\mathbf{I}| = 0$. As $\mathbf{T} = \mathbf{SU}$, we find

$$|\mathbf{T} - \lambda\mathbf{I}| = |\mathbf{S} - \lambda\mathbf{I}\mathbf{U}^{-1}||\mathbf{U}|. \tag{15}$$

$\mathbf{U}$ is a diagonal matrix so that $\det(\mathbf{U})$ is the multiplication of the diagonal elements, i.e.,

$$|\mathbf{U}| = \prod_{i=1}^{I} n_i \prod_{j=1}^{J} m_j. \tag{16}$$

Hence, it remains to calculate $|\mathbf{S} - \lambda\mathbf{U}^{-1}\mathbf{I}|$. Notice that $|\mathbf{S} - \lambda\mathbf{U}^{-1}\mathbf{I}|$ has a block matrix structure,

$$|\mathbf{S} - \lambda\mathbf{U}^{-1}\mathbf{I}| = \begin{vmatrix} \mathbf{A} & \mathbf{B} \\ \mathbf{C} & \mathbf{D} \end{vmatrix}, \tag{17}$$

where

$$\mathbf{A} = \underset{i=1,\ldots,I;\, j=1,\ldots,I}{a(i,j)} = \begin{cases} \left(\alpha\Gamma - \dfrac{\lambda}{n_i}\right) & \text{for } i = j, \\ \alpha\Gamma & \text{for } i \neq j; \end{cases} \qquad \mathbf{B} = \underset{i=1,\ldots,I;\, j=I+1,\ldots,I+J}{b(i,j)} = \Gamma p_i;$$

$$\mathbf{C} = \underset{i=I+1,\ldots,I+J;\, j=1,\ldots,I}{c(i,j)} = \Gamma p_i; \qquad \mathbf{D} = \underset{i=I+1,\ldots,I+J;\, j=I+1,\ldots,I+J}{d(i,j)} = \begin{cases} \left(\alpha\Gamma - \dfrac{\lambda}{n_i}\right) & \text{for } i = j, \\ \alpha\Gamma & \text{for } i \neq j. \end{cases}$$

For block matrices with $\det(\mathbf{A}) \neq 0$, the determinant is (see [10])

$$\det\begin{pmatrix} \mathbf{A} & \mathbf{B} \\ \mathbf{C} & \mathbf{D} \end{pmatrix} = \det(\mathbf{A})\det(\mathbf{D} - \mathbf{C}\mathbf{A}^{-1}\mathbf{B}). \tag{18}$$

Straightforward algebra gives

$$|\mathbf{S}-\lambda\mathbf{U}^{-1}\mathbf{I}| = (-\lambda)^{(I+J-2)}\left(\prod_{j=1}^{J}\frac{1}{m_j}\right)\left(\prod_{i=1}^{I}\frac{1}{n_i}\right) \times\left(\left(\alpha\Gamma\sum_{j=1}^{J}m_j-\lambda\right)\left(\alpha\Gamma\sum_{i=1}^{I}n_i-\lambda\right)-\Gamma^2\sum_{i=1}^{I}p_in_i\sum_{j=1}^{J}p_jm_j\right) \tag{19}$$

Hence, from (16) and (19)

$$|\mathbf{T}-\lambda\mathbf{I}| = |\mathbf{S}-\lambda\mathbf{I}\mathbf{U}^{-1}||\mathbf{U}| = \det(\mathbf{A})\det(\mathbf{D}-\mathbf{C}\mathbf{A}^{-1}\mathbf{B})\det(\mathbf{U}) = (-\lambda)^{(I+J-2)}F(\lambda), \tag{20}$$

where

$$F(\lambda) = \lambda^2-\lambda\alpha\Gamma\left(\sum_{i=1}^{I}n_i+\sum_{j=1}^{J}m_j\right)+\alpha^2\Gamma^2\sum_{i=1}^{I}n_i\sum_{j=1}^{J}m_j-\Gamma^2\sum_{i=1}^{I}p_in_i\sum_{j=1}^{J}p_jm_j \tag{21}$$

Clearly $|\mathbf{T}-\lambda\mathbf{I}|=0$ has $(I+J-2)$ zero eigenvalues and only two non-zero eigenvalues. These eigenvalues are determined from the solution of $F(\lambda)=0$. The Perron–Frobenius eigenvalue of $\mathbf{T}$ is the largest root of $F(\lambda)=0$. □

Thus, by discretizing the cell we obtain an explicit expression for the PF eigenvalue of $\mathbf{T}$ that can be used to characterize the feasibility of the downlink connection for a non-homogeneous distribution of calls over the segments. Using the explicit formulation of PF eigenvalue in Eq. (14), the feasibility of a user configuration $\mathbf{U}$ is now readily determined by checking the inequality $\lambda(\mathbf{U}) < s$. The set of all feasible user configurations is

$$\mathcal{S}_{\mathrm{D}} = \{\mathbf{U}|\lambda(\mathbf{U}) < s, \mathbf{U} =\in \mathbb{N}^{I+J}\}. \tag{22}$$

It can readily be shown that $\mathcal{S}_{\mathrm{D}}$ is a coordinate convex set, so that we may invoke the theory of loss networks [14] to characterize the distribution of non-persistent calls, which will be investigated in Section 3.2.

3.1.2. Uplink feasibility

Uplink feasibility via the PF eigenvalue of $\mathbf{H}$ was investigated in [8], where the condition

$$\mathbf{Z}^{\mathrm{U}} \geq 0 \text{ exist and } \mathbf{Z}^{\mathrm{U}} = (\mathbf{I}-\mathbf{H})^{-1}\mathbf{c} \Longleftrightarrow \rho(\mathbf{H}) < 1. \tag{23}$$

was used. An explicit expression for the PF eigenvalue, however, was not provided. Theorem 2 below provides this expression. As the proof is straightforward, it is omitted.

Theorem 2. *The Perron–Frobenius eigenvalue of* $\mathbf{H}$ *is*

$$\rho(\mathbf{H}) = \frac{\Gamma}{2}\left(\sum_{i=1}^{I}n_i-1+\sum_{j=1}^{J}m_j-1\right)+\frac{\Gamma}{2}\sqrt{\left(\sum_{i=1}^{I}n_i-\sum_{j=1}^{J}m_j\right)^2+4\sum_{i=1}^{I}p_in_i\sum_{j=1}^{J}p_jm_j}. \tag{24}$$

As in the downlink, we define the set of all feasible user configurations in the uplink. Thus, by developing a discretized cell model, we are able to derive an explicit formulation of PF eigenvalue not only for the downlink but also for the uplink. If we compare the downlink and uplink feasibility, we see that for the

expression for $\rho(\mathbf{H})$ is similar to $\lambda(\mathbf{T})$ for $\alpha = 1$. Thus, when there is no downlink interferences reduction, i.e., the non-orthogonality factor is equal to 1 or it is completely non-orthogonal, the interference in the downlink similar to the uplink.

Similar to the downlink, we define the set of all feasible user configurations in the uplink is

$$\mathcal{S}_{\mathrm{U}} = \{\mathbf{U} | \rho(\mathbf{U}) < 1, \mathbf{U} \in \mathbb{N}^{I+J}\}, \tag{25}$$

This is a also coordinate convex set.

3.2. Non-persistent calls: outage and blocking probabilities

We may distinguish two ways of handling fresh calls that bring the system in a non-feasible state: we may either block and clear the call from the system (*fresh call blocking*), or accept the call in which case the system is said to be in outage (*outage probability*) and (some) calls do not reach their energy per bit to interference threshold ϵ^*, until completion of some (other) call. These 'outage' and 'blocking' cases lead to different stochastic processes recording the number of calls in the segments.

When calls are blocked and cleared when the state is not feasible, the set of feasible states is the finite set $\mathcal{S}$ as defined in (22). Let $\{X(t), t \geq 0\}$ be the stochastic process recording the number of non-persistent and moving calls over the segments, which takes values in the finite state space $\mathcal{S}$. A state of the stochastic process is a vector $\mathbf{U} = (n_1, n_2, \ldots, n_I m_J, \ldots, m_2, m_1)$, that will be labelled as $\mathbf{U} = (u_1, u_2, \ldots, u_I u_{I+1}, \ldots, u_{I+J})$. When calls are not blocked, but instead all (or some) calls are in outage when the system state is not feasible, then all vectors in the positive orthant

$$\mathcal{S}^{\infty} = \{\mathbf{U} | \mathbf{U} = (\mathbf{N}, \mathbf{M}) \in \mathbb{N}^{I+J}\} \tag{26}$$

are possible system states. Let $\{X^{\infty}(t), t \geq 0\}$ be the corresponding stochastic process.

We are primarily interested in the distribution of calls over the segments $P(X^{\infty}(t) = \mathbf{U})$, and $P(X(t) = \mathbf{U})$. For the 'outage case' this distribution can be evaluated in closed form:

$$P(X^{\infty}(t) = \mathbf{U}) = \prod_{s=1}^{I+J} \mathrm{e}^{-\rho_s^{\infty}(t)} \frac{\rho_s^{\infty}(t)^{u_s}}{u_s!}, \tag{27}$$

where

$$\rho_s^{\infty}(t) = \tau \lambda_s(t) \tag{28}$$

is the time-dependent *load offered* to segment s: the distribution of the number of calls in cell s is Poisson with mean $\rho_s^{\infty}(t)$ proportional to the density of traffic and insensitive to the distribution of the call length G except through its mean τ, see [11] for a general framework for networks with unlimited capacity, and [21] for a derivation of the insensitivity result (27).

For the 'blocking case' the distribution $P(X(t) = \mathbf{U})$ cannot be obtained in closed form. However, for the regime of small blocking probabilities, the distribution $P(X(t) = \mathbf{U})$ can be adequately approximated using the modified offered load (MOL) approximation:

$$P(X(t) = \mathbf{U}) \approx P(X^{\infty}(t) = \mathbf{U} | X^{\infty}(t) \in \mathcal{S}) = \frac{\prod_{s=1}^{I+J} \mathrm{e}^{-\rho_s^{\infty}(t)} (\rho_s^{\infty}(t)^{u_s}/u_s!)}{\sum_{u \in \mathcal{S}} \prod_{s=1}^{I+J} \mathrm{e}^{-\rho_s^{\infty}(t)} (\rho_s^{\infty}(t)^{u_s}/u_s!)}.$$

The approximation is exact for a loss network in equilibrium. For networks with time-varying rates the MOL approximation is investigated in [12] for the Erlang loss queue, and is applied to networks of Erlang loss queues in [1]. It is shown that the error of the MOL approximation is decreasing with decreasing blocking probabilities and with decreasing variability of the arrival rate.

Outage and blocking probabilities are now readily obtained. First consider the 'outage case'. As the number of calls in the system increases, all calls suffer a gradual degradation of their QoS. If the energy per bit to interference ratio of a call falls below its target value ϵ^*, then the system is said to be in outage. The outage probability, $P_{\text{out}} = P(X^\infty(t) \notin \mathcal{S})$, is defined as the probability that an (instant) outage occurs to the system. The outage probability of a user in segment j in a cell can be formulated as follows:

$$P_{\text{out}} = P(\epsilon_j < \epsilon^* \text{ for some } j). \tag{29}$$

The outage probability cannot be evaluated in closed form due to the complexity of the feasible set $\mathcal{S}$, and will be evaluated via Monte-Carlo simulation.

For the 'blocking case', the fresh call blocking probability must be determined per segment. To this end, define the blocking set of segment k as $\mathcal{S}_k = \{\mathbf{U} \in \mathcal{S} | \lambda(\mathbf{U} + \mathbf{e}_k) > s\}$ where $\mathbf{e}_k$ is the unit vector with entry k equal 1, and all other entries 0. Then, as is shown in [1], the blocking probability, $B_k(t)$, of a segment k at time t is approximated as

$$B_k(t) \approx P(X^\infty(t) \in \mathcal{S}_k | X^\infty(t) \in \mathcal{S}) = \frac{\sum_{\mathbf{U}\in\mathcal{S}_k} \prod_{s=1}^{I+J} \mathrm{e}^{-\rho_s^\infty(t)} (\rho_s^\infty(t)^{u_s}/u_s!)}{\sum_{u\in\mathcal{S}} \prod_{s=1}^{I+J} \mathrm{e}^{-\rho_s^\infty(t)} (\rho_s^\infty(t)^{u_s}/u_s!)}.$$

The blocking probability cannot be evaluated in closed form due to the complexity of the feasible set $\mathcal{S}$, and will be valuated via Monte-Carlo simulation.

4. Downlink rate optimization

This section presents a model for system utility optimization based on the feasibility model. In particular, the objective is to find the best border location for both downlink and uplink that maximizes the total number of uplink users and maximizes the total downlink rate.

4.1. Uplink and downlink feasibility

Recall the feasibility condition for downlink and uplink, in (12) and (23) resp. Feasibility of power control allocations have been investigated via PF eigenvalues. We are interested in feasibility when the rate and the users distributions are not fixed. Given (14) and (24), the feasibility conditions in (12) and (23) can be rewritten as

$$\lambda'(n_i, m_j, R_{\text{D}}) < \frac{2W}{\epsilon_{\text{D}}^*}, \tag{30}$$

$$\rho'(n_i, m_j, R_{\text{U}}) < \frac{2W}{\epsilon_{\text{U}}^*}, \tag{31}$$

where

$$\lambda'(n_i, m_j, R_{\mathrm{D}}) = R_{\mathrm{D}} \left(\alpha \left(\sum_{i=1}^{I} n_i + \sum_{j=1}^{J} m_j - 2 \right) + \sqrt{\alpha^2 \left(\sum_{i=1}^{I} n_i - \sum_{j=1}^{J} m_j \right)^2 + 4 \sum_{i=1}^{I} p_i n_i \sum_{j=1}^{J} p_j m_j} \right), \tag{32}$$

$$\rho'(n_i, m_j, R_{\mathrm{U}}) = R_{\mathrm{U}} \left(\left(\sum_{i=1}^{I} n_i + \sum_{j=1}^{J} m_j - 2 \right) + \sqrt{\left(\sum_{i=1}^{I} n_i - \sum_{j=1}^{J} m_j \right)^2 + 4 \sum_{i=1}^{I} p_i n_i \sum_{j=1}^{J} p_j m_j} \right). \tag{33}$$

Eqs. (30) and (31) represent the feasibility condition for downlink and uplink where the system parameters W, ϵ_{D}^* and ϵ_{U}^* are fixed. Using those expressions, we investigate the relation between user distribution (n_i, m_j), uplink rate R_{U} and downlink rate R_{D}. We observe that for $\alpha = 1$, the expression for downlink feasibility and uplink feasibility are the same. Moreover, since the downlink non-orthogonality factor has a value between 0 and 1, i.e., $0 \leq \alpha \leq 1$, for the case of $R_{\mathrm{D}} = R_{\mathrm{D}} = R$ we always have the following relation:

$$\lambda'(n_i, m_j, R) \leq \rho'(n_i, m_j, R) \tag{34}$$

This means that the downlink rate can be upgraded while maintaining both uplink and downlink feasibility.

4.2. Border optimization

From (14) and (24), we observe that the PF eigenvalues can be related to the border location. This is done by assigning users from a cell to other cells, i.e., assigning I and J given users distribution $\mathbf{U} = (n_1, n_2, \ldots, n_I, m_J, \ldots, m_2, m_1)$. We observe that the downlink PF eigenvalue decreases as the location of the border is located further from the middle of the traffic burst. Therefore, it seems optimal to handle all calls in a single BTS. While in the uplink, the uplink PF eigenvalue decreases as the border is located closer to the middle of the traffic burst. So, from the uplink point of view, it is optimal to equally divide calls over two BTSs. From those two observations, we see that there is a trade-off between uplink and downlink optimal border location. Therefore the border location should be determined by considering both downlink and uplink properties. We formulate an optimization problem to solve the combined downlink-uplink optimal border location in this section.

The arguments above suggest that the optimal downlink rate assignment may be to assign rate zero to all segments except for the segment closest to a BTS. This is clearly not a practical solution. Therefore, in our optimization problem, we add a practical constraint that the number of segments with non-zero rates assignment should be maximized. This means that the rate assignment is fair in the sense that the

maximum number of calls is carried with equal rate. The combined optimization problem is formulated as follows:

$$\begin{cases} \text{Find borders locations, } I \text{ and } J, \text{ and downlink rate } R_{\mathrm{D}} \text{ that maximize the system utility and} \\ \text{number of carried calls} \\ \text{s.t. uplink feasible \& downlink feasible.} \end{cases} \tag{35}$$

In this paper, the coverage of a cell is equal to the number of segments covered by the cell. Thus, the border of cell X is defined as the point located after segment I and the border of cell Y is defined as the point located after segment J. Using the feasibility conditions expression in (32) and (33), the problem can be formulated as follows:

$$\begin{aligned} &\max_{R_{\mathrm{D}},I,J} R_{\mathrm{D}} \left(\sum_{i=1}^{I} n_i + \sum_{j=1}^{J} m_j \right) \\ &\text{s.t} \quad \lambda'(n_i, m_j, R_{\mathrm{D}}) < \frac{2W}{\epsilon_{\mathrm{D}}^*} \\ &\qquad I, J \in \arg\max \left(\sum_{i=1}^{I} n_i + \sum_{j=1}^{J} m_j \right) \\ &\qquad\qquad \text{s.t} \quad \rho'(n_i, m_j, R_{\mathrm{U}}) < \frac{2W}{\epsilon_{\mathrm{U}}^*} \\ &\qquad\qquad i = 1, 2, \ldots, I; \quad j = 1, 2, \ldots, J \\ &\qquad\qquad I + J \le K \end{aligned} \tag{36}$$

where K is the total number of segments. Note that the constraints are non-convex functions in n_i and m_j. Hence, the optimization problem above is not easy to solve. We propose a decomposition algorithm to solve the optimization problem. From (34), we learn that $(\sum_{i=1}^{I} n_i + \sum_{j=1}^{J} m_j)$ in the objective function is mainly determined by the uplink. Hence to find the optimal solution $(I^*, J^*, R_{\mathrm{D}}^*)$ of the problem above, we construct the following algorithm:

1. First, given the traffic load, we label the number of users in each segment as $U = (u_1, u_2, \ldots, u_k, \ldots, u_K)$, where K is the total number of segments.
2. Next, we assign users for a certain border location. For this purpose, we define an initial border at segment k, $k = 1, 2, \ldots, K$. By putting the initial border at segment k, this means that we assign users in the first k segments to cell X and the next $(K - k)$ segments to cell Y, i.e.,

$$(n_i^k, m_j^k) = \begin{cases} n_i = u_i, & i = 1, 2, \ldots, k, \\ m_j = u_{K-(j-1)}, & j = (k+1), \ldots, K, \end{cases}$$

where (n_i^k, m_j^k) denote the set of assigned users when the initial border located at segment k, $k = 1, 2, \ldots, K$. We denote the initial border as (I_k^0, J_k^0).

3. Next, we check the uplink feasibility given the initial border at segment k, (I_k^0, J_k^0), and the assigned users (n_i^k, m_j^k), $k = 1, 2, \ldots, K$. We check the an uplink feasibility given by the first constraint, i.e.,

$$\rho''(n_i^k, m_j^k) < \frac{2W}{\epsilon_{\mathrm{U}}^* R_{\mathrm{U}}}, \tag{37}$$

where $\rho''(n_i, m_j) = \rho'(n_i, m_j, R_{\mathrm{U}})/R_{\mathrm{U}}$ derived from (33), i.e.,

$$\rho''(n_i^k, m_j^k) = \left(\sum_{i=1}^{I_k^0} n_i^k + \sum_{j=1}^{J_k^0} m_j^k - 2\right) + \sqrt{\left(\sum_{i=1}^{I_k^0} n_i^k - \sum_{j=1}^{J_k^0} m_j^k\right)^2 + 4\sum_{i=1}^{I_k^0} p_i n_i^k \sum_{j=1}^{J_k^0} p_j m_j^k}. \tag{38}$$

Thus, given the set of users (n_i^k, m_j^k) and the initial border set (I_k^0, J_k^0), the uplink feasibility is checked as follows:

$$\rho''(n_i^k, m_j^k) \begin{cases} \text{if } < \dfrac{2W}{\epsilon_{\mathrm{U}}^*} \text{ then the border is } (I_k^0, J_k^0), \\ \text{if } \geq \dfrac{2W}{\epsilon_{\mathrm{U}}^*} \text{ then drop segments until feasible.} \end{cases}$$

The dropped segment is the one that contributed at most to $\rho''(n_i^k, m_j^k)$. From (38), we can see that the dropped segment is located close to the cell border. If we drop the segment $J_k = J_k^0$, then we set $I_k' = k$ and $J_k' = (K - k - 1)$. If we drop the segment $I_k = I_k^0$, then we set $I_k' = (k - 1)$ and $J_k' = (K - k)$. Then, we obtain a set of border (I_k, J_k) with a gap of a segment. We repeat those steps until (37) is satisfied. Finally, for each k, we obtain a set of border $B_k = (I_k, J_k)$ that supports a maximum number of users, $U_k = (n_i^k, m_j^k)$, under uplink feasibility constraints.

4. Next, we determine a set of $B_k = (I_k, J_k)$, $k = 1, 2, \ldots, K$, that maximize $(\sum_{i=1}^{I_k} n_i^k + \sum_{j=1}^{J_k} m_j^k)$. Thus, given the border B_k from step 3, we choose k^* among all k, the set that gives either optimal carried calls, $(\sum_{i=1}^{I_k} n_i^k + \sum_{j=1}^{J_k} m_j^k)$ or optimal carried segments $(I_k + J_k)$.
Denote the sets of optimal borders determined by the carried call as $O^{\mathrm{U}} = \{B_{k1}^{\mathrm{U}}, B_{k2}^{\mathrm{U}}, \ldots, B_{kq}^{\mathrm{U}}\}$. Denote the sets of optimal borders determined by the carried segment as $O^{\mathrm{S}} = \{B_{k1}, B_{k2}^{\mathrm{S}}, \ldots, B_{kr}^{\mathrm{S}}\}$.
5. Given the set border locations that support maximum number of uplink feasible users, i.e., the set O^{U} and O^{S}, we determine the maximal downlink rate

$$R_{\mathrm{D}} < \frac{2W}{\epsilon_{\mathrm{D}}^*(\lambda''(n_i^k, m_j^k, I_k, J_k))}, \tag{39}$$

where

$$\lambda''(n_i, m_j, I, J) = \alpha\left(\sum_{i=1}^{I} n_i + \sum_{j=1}^{J} m_j - 2\right) + \sqrt{\alpha^2\left(\sum_{i=1}^{I} n_i - \sum_{j=1}^{J} m_j\right)^2 + 4\sum_{i=1}^{I} p_i n_i \sum_{j=1} J p_j m_j}. \tag{40}$$

Thus we obtain a set from O^{U}, i.e.,

$$P^{\mathrm{U}} = \{(B^{\mathrm{U}}_{k1}, R^{\mathrm{U}}_{\mathrm{D}1}), (B^{\mathrm{U}}_{k}, R^{\mathrm{U}}_{\mathrm{D}2}), \ldots, (B_k, R^{\mathrm{U}}_{\mathrm{D}})\}$$

and a set from U^{S}, i.e.,

$$P^{\mathrm{S}} = \{(B^{\mathrm{S}}_{k1}, R^{\mathrm{S}}_{\mathrm{D}1}), (B^{\mathrm{S}}_{k2}, R^{\mathrm{S}}_{\mathrm{D}2}), \ldots, (B^{\mathrm{S}}_{k2}, R^{\mathrm{S}}_{\mathrm{D}r})\}.$$

6. Finally, we determine the maximal value of $R_{\mathrm{D}}(\sum_{i=1}^{I_k} n_i^k + \sum_{j=1}^{J_k} m_j^k)$. This is done by checking all k in the sets P^{U} and P^{S}.

The above algorithm is numerically illustrated in the next section.

5. Numerical results

In this section, we give some numerical examples demonstrating the results of our model. First, we investigate the relation between downlink performance and downlink border location. Second, we consider downlink border optimization under uplink coverage restrictions.

The parameters that are used for this numerical results are those provided in [9]: the system chip rate $W = 3.84$ MHz, the required energy per bit to interference ratio $\epsilon^* = 5$ dB, the downlink non orthogonality factor $\alpha = 0.3$, and the path loss exponent $\gamma = 4$. The distance between the two BTSs X and Y is 2000 m, divided into 40 segments of width 50 m. We assume that all terminals use the same uplink rate $R_{\mathrm{U}} = 32$ kbps. For the downlink, we assume that initially all terminals use the same downlink rate $R_{\mathrm{D}} = 32$ kbps. Additional results for a system with lower rates $R_{\mathrm{U}} = R_{\mathrm{D}} = 12.2$ kbps and lightly loaded non-hot spot cells are provided in [6].

5.1. Downlink performance

This section investigates the downlink performance, i.e., the outage probability and the blocking probability per segment, for the case of fixed border and moving border. In the first case, we investigate the downlink performance for a moving traffic hot spot for fixed border location. The performance is calculated as a function of the location of the traffic. In the second case, we investigate the downlink optimal border for non-moving traffic. The performance is calculated as a function of the border location. We will investigate results from Monte-Carlo simulation, and a prediction based on the Perron–Frobenius eigenvalue obtained from the offered load in the segments. Sufficient samples are generated to have 95% confidence and 10% relative precision. To facilitate a graphical representation of our results, we will depict blocking probabilities only for those time instances at which the hot spot enters a new segment.

5.2. Location of the hot spot: traffic types

Throughout this section, we assume that a block shaped traffic jam of width 10 segments moves from BTS X to BTS Y at constant speed, see Fig. 2. The load in segments inside the hot spot is 5 Erlangs. The

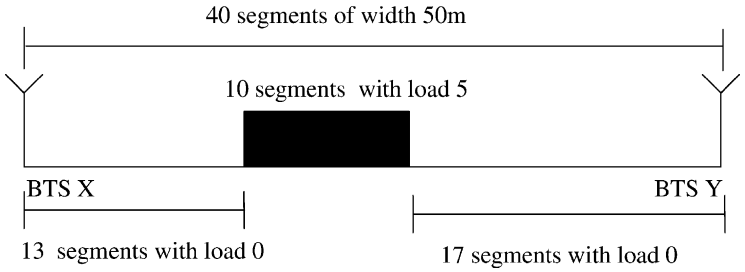

Fig. 2. Rectangular hot spot.

location of the hot spot after the $(12 + i)$th segment from BTS X will be referred to as type i traffic load, i.e. Fig. 2 depicts type 1 traffic. In our numerical results we will only consider types $1, \ldots, 5$, as the hot spot location in the area roughly in the middle between the BTSs is most interesting. Notice that type 5 is the mirror image of type 1, with 13 segments between the hot spot and BTS Y.

5.2.1. First case: fixed border, moving traffic

First consider the commonly studied case of a fixed border located in the middle between the BTSs, i.e. each cell consists of 20 segments. Blocking and outage probabilities can be obtained via Monte-Carlo simulation. Below we will numerically investigate the blocking probabilities per segment for a moving hot spot. Fig. 3 depicts the outage and total blocking probabilities for traffic types 1–5, where the total blocking is the fraction of blocked fresh calls over the entire area between BTSs X and Y. Both the outage and the total blocking probability do not discriminate between segments. Clearly, type 3 traffic with the hot spot located in the middle between BTSs yields the largest value for the blocking probabilities, in accordance with intuition. Fig. 4 depicts blocking probabilities per segment for traffic types 1–5, that is the fraction of blocked fresh calls counted for each segment separately. As can be seen from the graph, when the hot spot is located more to the left, the blocking probability of the segments in the right is higher (see types 1 and 2 traffic load) and vice versa. The type 3 case is symmetric. This result shows that as the traffic jam moves closer to the border, the downlink performance gets worse. The result suggests that it is optimal for the downlink to have all calls located in the same cell. This motivates an investigation of the downlink performance when the border is not fixed.

5.2.2. Second case: moving border, non-moving traffic

Let us now investigate the optimal location of the border between the cells for a given traffic pattern, i.e., the location of the border that gives the best downlink performance. For this case, we consider the traffic of type 1. Fig. 5 depicts the downlink PF eigenvalue λ as a function of the offered load only. The graph has a clear peak for a cell border between roughly 700 and 1100 m from BTS X. As the feasibility criterion is $\lambda < s$ (recall (12)), from the curve it seems optimal for the cell border to be such that the entire hot spot resides in a single cell. Monte-Carlo simulation of the blocking probabilities per segment for type 1 traffic and different locations of the border at 700, 900, 1000 m from BTS X as depicted in Fig. 6 support this observation: congestion in the downlink can be reduced by allocating the entire traffic burst into one cell.

The conclusion of this section, based on the downlink only, is in clear contrast with the well-known uplink result that indicates that the load should be evenly divided over the cells. Thus, there is a trade-off

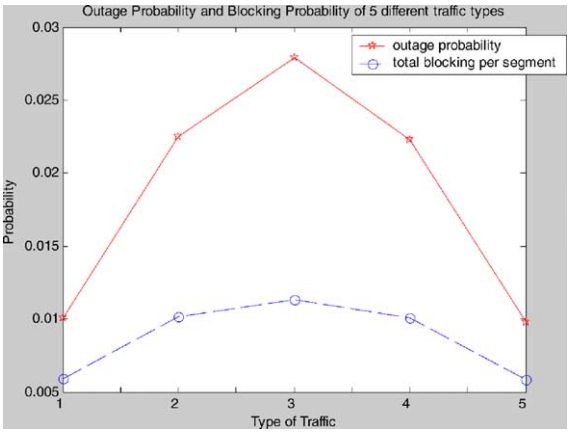

Fig. 3. Outage and total blocking.

between downlink congestion and uplink congestion: the location of the border should be determined by considering both uplink and downlink.

5.3. Border optimization

5.3.1. Persistent calls

This section investigates the optimal border location based on the optimization problem of Eq. (36). In the first case, we fix the traffic load to be of type 1 as in Fig. 2. This algorithm (in steps 1–3) first investigates the possible border locations that give the optimal number of carried calls or carried segments.

Fig. 7 depicts the optimal border locations, $B_k = (I_k^*, J_k^*)$, as a function of the initial border location placed at segment k. Thus, the optimal cell borders (step 4) are $O^{\mathrm{U}} = O^{\mathrm{S}} =$

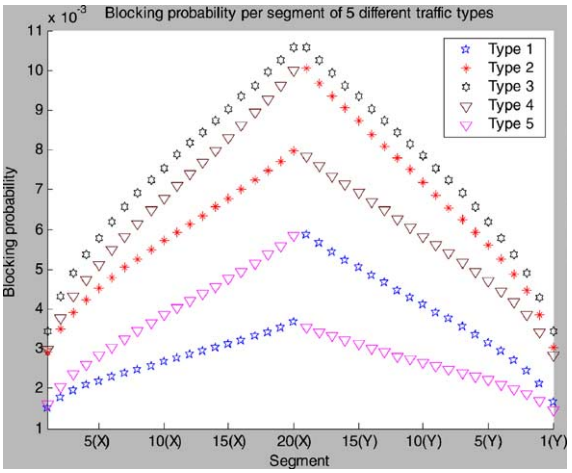

Fig. 4. Blocking per segment.

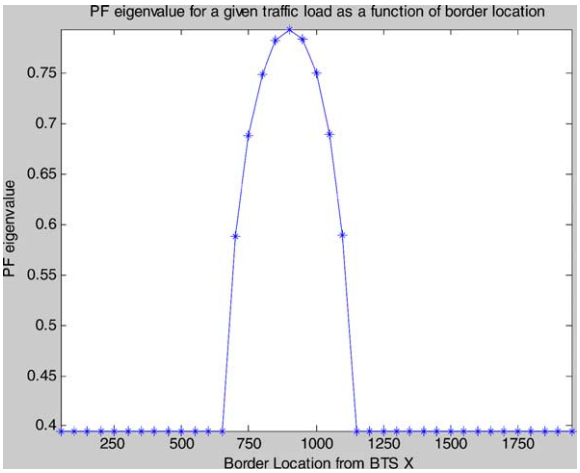

Fig. 5. Downlink PF eigenvalue.

$\{(U_{15}, B_{15}), (U_{16}, B_{16}), \ldots, (U_{22}, B_{22})\}$ obtained for k between 15 and 22, as indicated by the vertical lines in Fig. 7. Notice that there is coverage gap in the middle between BTS X and Y.

Given the optimal set of carried segments O^{S}, step 5 of the algorithm determines the possible upgrade of downlink rate R_{D} using Eq. (39). Fig. 8 depicts the utility function $R_{\mathrm{D}}(\sum_{i=1}^{I_k} n_i^k + \sum_{j=1}^{J_k} m_j^k)$ as a function of k. The maximal utility value is denoted as star in Fig. 8. Thus, the border location that gives maximal utility is at $k = 22$. The optimal border location for cell X is at $I = 21$ (950 m from BTS X) and the optimal border location for cell Y is at $J = 18$ (950 m from BTS Y). The maximum is obtained with the border located further from the center of the hot spot/traffic burst: maximal system utility is obtained by putting the borders such that most of the traffic is covered in a single cell.

Notice from Fig. 8 that the system utility can be increased when we let the system support less carried calls, in this case the per call downlink rate is higher, but the number of carried calls is lower. This shows

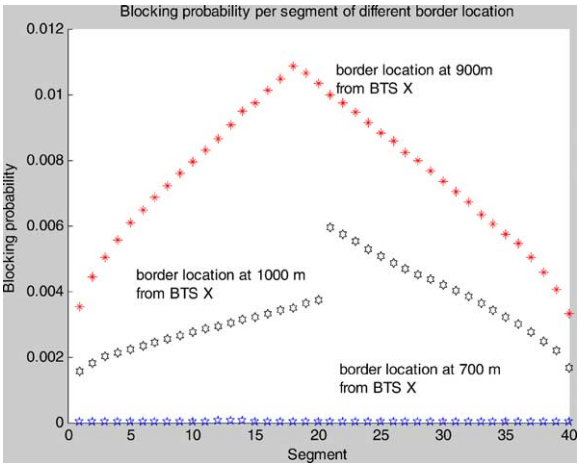

Fig. 6. Blocking per segment.

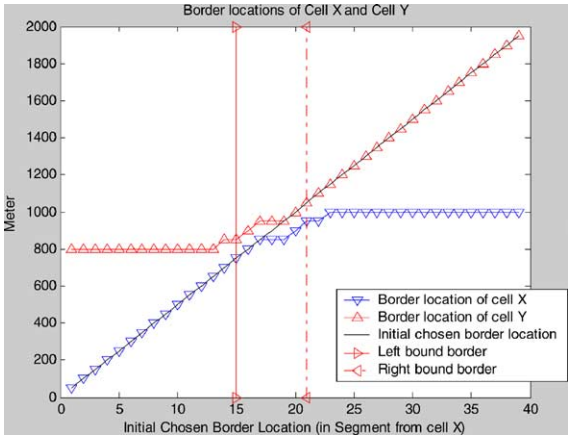

Fig. 7. Optimal border location.

the fairness trade-off between number of carried calls and the system utility: by serving less calls the remaining calls would be able to achieve higher total utility. A similar result is found in [18], where the uplink is investigated, only.

Next, we investigate the optimal border location for the case of moving traffic. The objective is to understand the optimal border location and its optimal system utility. For this purpose, we let the hot spot of type 1 (see Fig. 2) moves from BTS *X* to BTS. In this example, we consider only five steps. For each step, we investigate the optimal border location that gives maximal utility. Fig. 9 depicts the optimal border locations in each step that gives the maximum system utility and illustrates that in this numerical example there is no distinction made in our algorithm using the optimal number of carried calls and the optimal number of carried segments. Fig. 10 depicts that the maximum system utility based on carried calls and the the maximum system utility based on carried segments. As the traffic burst moves closer

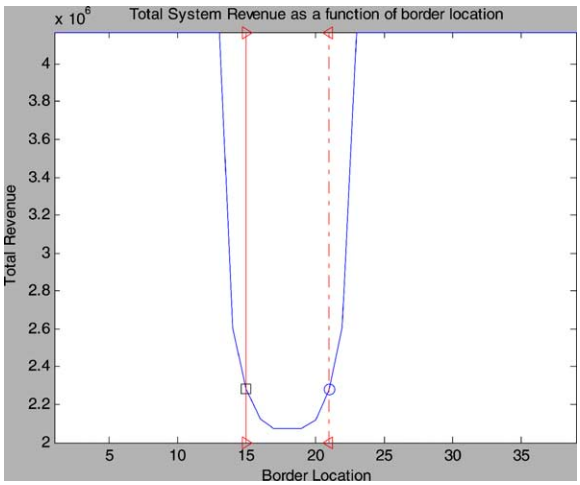

Fig. 8. Perron–Frobenius eigenvalue.

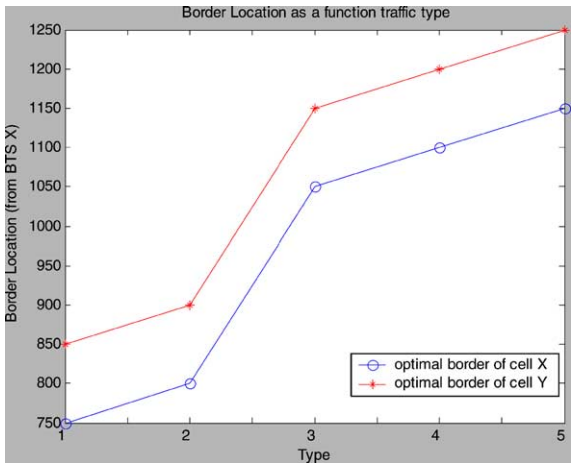

Fig. 9. Optimal border location.

to the middle of the cell, the optimal total revenue decreases. Furthermore, Fig. 10 indicates that it is optimal to choose the border location such that most of the traffic burst is covered by a single cell.

5.3.2. Non-persistent calls

Now, we investigate the optimal border location for the case of non-persistent calls by Monte-Carlo simulation for traffic type 1 (see Fig. 2). For each realization, we perform the algorithm in Section 4.2.

Fig. 11 depicts the probability that we obtain a location of the border in a particular place. The figure shows that there are two peaks for the border of cell *X*, i.e., at 650 and 1000 m, and by symmetry also two peaks for the border of cell *Y*, i.e., at 800 m and at 1150 m. The peak at 650 m for cell *X* is dominant. This is in contrast with the result for persistent calls. The discrepancy is due to the algorithm, that starts including calls in cell *X* from the left. In the case of a tie in revenue, it chooses the left border thus favouring the left border location. These results show that also in the case of non-persistent calls the optimal border

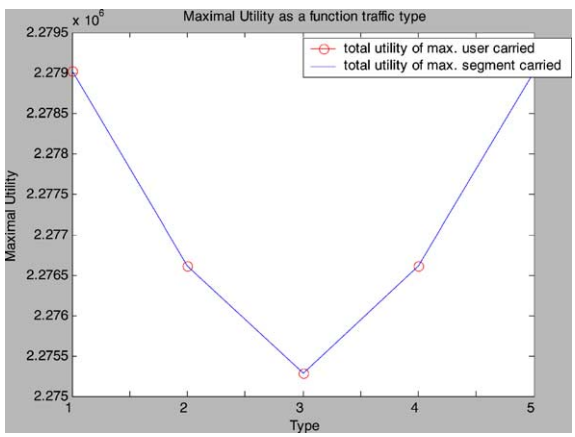

Fig. 10. Optimal system utility.

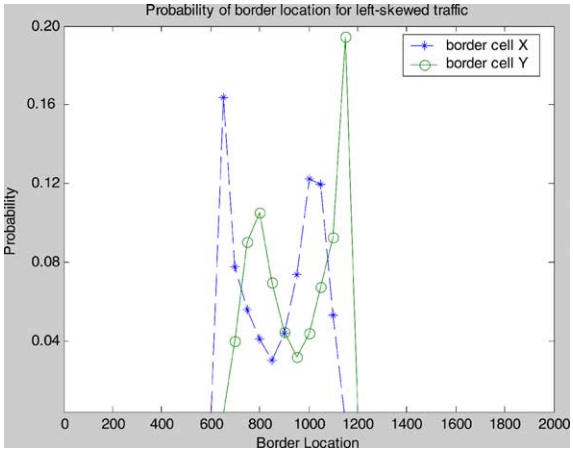

Fig. 11. Simulated border location for left-skewed traffic.

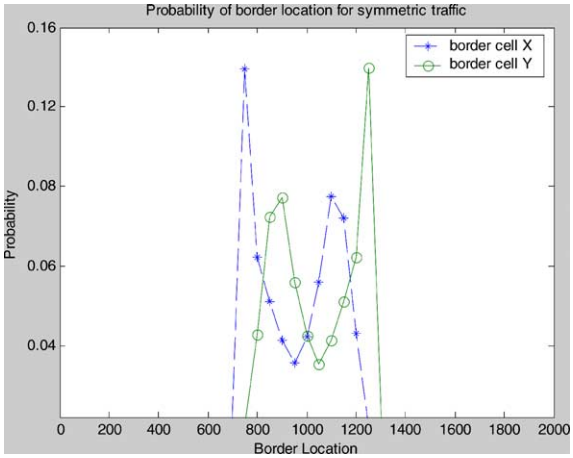

Fig. 12. Simulated border location for symmetric traffic.

location includes most of the traffic burst in a single cell, i.e., either in cell *X* or in cell *Y*. This is more clearly visible in Fig. 12 that depicts the optimal border location for symmetric traffic (Type 3), i.e., in the setting of non-persistent calls when two boundary locations around 750 and 1250 m yield the same revenue, the algorithm selects the boundary at 750 m.

From those two examples, we can conclude that the optimal system revenue, i.e., with maximal number of uplink users and maximal downlink rate, is obtained by covering most of the traffic in a single cell.

6. Conclusion

This paper has provided a model for characterizing downlink and uplink power assignment feasibility. We have obtained an explicit decomposition of system and user characteristics, and have provided an

explicit analytical expression for the Perron–Frobenius eigenvalue that determines feasibility and blocking probabilities. Based on this result we have numerically investigated blocking probabilities and found for the downlink that it is best to allocate all calls to a single cell. When also taking the uplink that determines coverage into account, we have developed a downlink rate optimization algorithm and have investigated the optimal cell border based on both uplink and downlink interference. The results indicate that the optimal border location that maximizes the system utility (downlink rate) can be obtained by including most of the carried traffic into a single cell.

Acknowledgements

The research is partly supported by the Technology Foundation STW, Applied Science Division of NWO and the Technology Programme of the Ministry of Economic Affairs, The Netherlands. The authors would like to thank Adriana Bumb for interesting and insightful discussions.

References

[1] N. Abdalla, R.J. Boucherie, Blocking probabilities in mobile communications networks with time-varying rates and redialing subscribers, Ann. Operations Res. 112 (2002) 15–34.
[2] N. Bambos, S.C. Chen, G. Pottie, Channel access algorithms with active link protection for wireless communication networks with power control, IEEE/ACM Trans. Netw. 8 (5) (2000) 583–597.
[3] D. O'Neill, D. Julian, S. Boyd, Seeking Foschini's genie: optimal rates and powers in wireless networks, IEEE Trans. Vehicular Technol., in press.
[4] X. Duan, Z. Niu, J. Zheng, Downlink transmit power minimization in power-controlled multimedia Cdma systems, in: Proceedings of the 2002 International Symposium on Personal, Indoor and Mobile Radio Communications (PIMRC'02), September 2002.
[5] X. Duan, Z. Niu, D. Huang, D. Lee, A dynamic power and rate joint allocation for mobile multimedia DS-CDMA network based on utility functions, in: Proceedings of the 2002 International Symposium on Personal, Indoor and Mobile Radio Communications (PIMRC'02), September 2002.
[6] A.I. Endrayanto, J.L. van den Berg, R.J. Boucherie, An analytical model for CDMA downlink rate optimization taking into account uplink coverage restrictions, Memorandum No. 1699, Department of Applied Mathematics, University of Twente, 2003.
[7] J.S. Evans, D. Everitt, Effective bandwidth-based admission control for multiservice CDMA cellular networks, IEEE Trans. Vehicular Technol. 48 (1999) 36–46.
[8] S.V. Hanly, Congestion measures in DS-CDMA networks, IEEE Trans. Commun. 47 (3) (1999) 426–437.
[9] H. Holma, A. Toskala, WCDMA for UMTS, Wiley, New York, 2000.
[10] C. Meyer, Matrix Analysis and Applied Linear Algebra, SIAM, Philadelphia, 2000.
[11] W.A. Massey, W. Whitt, Networks of infinite-server queues with nonstationary Poisson input, Queueing Syst. 13 (1993) 183–250.
[12] W.A. Massey, W. Whitt, An analysis of the modified offered load approximation for the nonstationary Erlang loss model, Ann. Appl. Prob. 4 (1994) 1145–1160.
[13] G.F. Newell, A simplified theory of kinematic waves in highway traffic, part I: General theory, Transport. Res. 27B (1993) 281–287.
[14] K.W. Ross, Multiservice Loss Networks for Broadband Telecommunications Networks, Springer, Berlin, 1995.
[15] D. Saban, J.L. van den Berg, R.J. Boucherie, A.I. Endrayanto, CDMA coverage under mobile heterogeneous network load, in: Proceedings of 2002 IEEE 56th Vehicular Technology Conference, VTC 2002-Fall, Vancouver, Canada, 2002.
[16] E. Seneta, Non-Negative Matrices, Allen and Unwin, London, 1973.

[17] K. Sipilä, et al., Estimation of capacity and required transmission power of WCDMA based on downlink pole equation, in: Proceedings of VTC 2000, vol. 2, Tokyo, 2002, pp. 1002–1005.
[18] V.A. Siris, Cell coverage based on social welfare maximization, in: Proceedings of IST Mobile and Wireless Telecommunications Summit, Greece, June 2002.
[19] A. Sampath, P. Kumar, J. Holtzman, Power control and resource management for a multimedia wireless CDMA system, in: Proceedings of the 1995 International Symposium on Personal, Indoor and Mobile Radio Communications (PIMRC'95), September 1995.
[20] D. Staehle, et al., Approximating the othercell interference distribution in inhomogeneous UMTS networks, in: Proceedings of the IEEE Vehicular Technology Conference (VTC-02 Spring), Birmingham, AL, 2002.
[21] A. Ule, R.J. Boucherie, Adaptive dynamic channel borrowing in road-covering mobile networks, Memorandum No. 1589, Department of Applied Mathematics, University of Twente, 2001.
[22] M. Xiao, N.B. Shroff, E.K.P. Chong, Utility-based power control in cellular wireless systems, in: Proceedings of IEEE INFOCOM, 2001.

A. Irwan Endrayanto is a PhD candidate at Stochastic Operation Research Group, Department of Applied Mathematics, University of Twente. He received his Bachelor's degree in Mathematics at Gadjah Mada University, Indonesia in 1996, and his Master of Science in Engineering Mathematics' degree at Department Applied Mathematics, University of Twente in 2000. His current research topic is dynamic capacity allocation in wireless networks.

Hans van den Berg received the MSc and PhD degree in Mathematics from the University of Utrecht, The Netherlands, in 1986 and 1990, respectively. From 1986, he worked at the Centre for Mathematics and Computer Science (CWI), Amsterdam. In 1990, he joined KPN Research, Leidschendam, The Netherlands, as a member of technical staff in the Department Network Planning. Since 1997, he is a Senior Research Member and is currently leader of the QoS group within TNO Telecom, Delft, The Netherlands. He is particularly working on performance modelling, evaluation and dimensioning of fixed and mobile communication networks. In these fields, he has co-operated within many international projects, e.g. in the European RACE, ACTS and COST research programmes. Since July 2003 he has a part-time professorship within the Department of Computer Science, University of Twente, The Netherlands.

Richard J. Boucherie is full professor of stochastic processes in telecommunications and logistics at the Department of Applied Mathematics of the University of Twente. He studied applied mathematics and theoretical physics at the University of Leiden, and received his PhD from the Vrije Universiteit, Amsterdam in 1992 for a thesis on product-form in queueing networks. Currently, Richard's research interests are in stochastic processes such as Petri nets and queueing networks, and their application to capacity allocation and data services in mobile telecommunications systems and logistics.